Characterization of Mg^{2+}-Dependent 3′-Processing Activity for Human Immunodeficiency Virus Type 1 Integrase *in Vitro*: Real-Time Kinetic Studies Using Fluorescence Resonance Energy Transfer†

S. Paul Lee, Hyung G. Kim, Michael L. Censullo, and Myun K. Han*

Department of Biochemistry and Molecular Biology, Georgetown University Medical Center, Washington, D.C. 20007

Received January 25, 1995; Revised Manuscript Received April 12, 1995®

ABSTRACT: Human immunodeficiency virus type 1 integrase (HIV-1 IN) catalyzes the integration of HIV-1 DNA into the host chromosome. *In vitro* reactions with endogenous viral DNA require Mg^{2+} as the metal cofactor, whereas *in vitro* studies performed with short oligonucleotide substrates utilize Mn^{2+}. In this study, we report that the donor processing activity of HIV-1 IN alters depending on the structure and length of the oligonucleotide substrates. Increases in the length of the substrate cause alterations in the efficiency of Mg^{2+}-dependent donor processing activity, thereby reconciling this discrepancy between the *in vivo* and *in vitro* HIV-1 IN mediated reactions. We have also found that the 3′-processing activity of HIV-IN is responsible for cleaving the junction between the viral and target sequences of the recombination intermediate. Its mechanism differs from the previously described disintegration reaction in that the donor strands are regenerated without a joining reaction of the target strands. Kinetic studies of 3′-processing activity suggest that the k_{cat} (0.24/h) is very low. This implies that HIV-1 IN remains as a complex with the processed DNA prior to the strand transfer reaction.

Retroviral integration is an essential step in the retrovirus life cycle and has increasingly become an attractive target in the development of antiviral drugs. Human immunodeficiency virus type 1 (HIV-1)[1] integrase, encoded by the viral *pol* gene, is responsible for catalyzing the integration of HIV-1 DNA into the host chromosome. Integration requires specific sequences at the ends of the linear double-stranded viral DNA that are synthesized by reverse transcription from the viral RNA genome in infected cells (Varmus & Brown, 1989; Grandgenett & Mumm, 1990; Katz & Skalka, 1994). *In vitro* studies using double-stranded short oligonucleotides corresponding to either the U5 and U3 ends of viral DNA and purified IN expressed in bacteria provide genetic evidence for the viral DNA integration reaction being mediated entirely by the IN enzyme (Brown et al., 1989; Katzman et al., 1989; Fujiwara & Craigie, 1989; Katz et al., 1990; Vora et al., 1990; Craigie et al., 1990; Sherman & Fyfe, 1990; Bushman & Craigie, 1991).

Upon recognition of a specific DNA sequence within both ends of the long terminal repeat (LTR) of viral DNA, two terminal nucleotides at the 3′ ends of both LTR are removed by IN in the cytoplasm (3′-processing; Sherman & Fyfe, 1990; Bushman & Craigie, 1991; Katzman et al., 1989; Pauza, 1990). Subsequently, the recessed CA_{OH}-3′ end is then joined to the 5′ end of the chromosomal target DNA, producing a hybrid strand in the nucleus (strand transfer). The 3′ end of the cleaved target DNA remains unjoined and a Y-shaped gapped recombination intermediate is produced (Figure 1). Recent mechanistic studies of 3′-processing and strand transfer reactions suggest that integration occurs as a one-step reaction (Engelman et al., 1991) without a requirement for an exogenous energy source (Bushman et al., 1990; Farnet & Haseltine, 1990; Ellison et al., 1990). Thus, the target DNA does not need to be cut by the viral integrase but is joined to the viral DNA by a concerted phosphoryl transfer. To complete the integration process, the gapped intermediate is then repaired by a process that remains to be elucidated. Further *in vitro* studies of an oligonucleotide substrate that mimics the Y-shaped gapped recombination intermediate have shown that integrase can also promote a reaction termed disintegration (Chow et al., 1992; Vincent et al., 1993). In this reaction both the precursor viral DNA and the target strand are regenerated by a cutting−joining reaction of the recombination intermediate.

A problem cited with the currently available *in vitro* assays is that there are often discrepancies between the results obtained with the short oligonucleotide substrates usually employed and those obtained from infected cell extracts utilizing endogenous viral DNA. *In vitro* experiments with short substrates show that 3′ donor processing and strand transfer reactions are not observed with Mg^{2+} as the divalent cation (Sherman & Fyfe, 1990; Craigie et al., 1990), whereas the recessed ends of the endogenous viral DNA within core particles integrate efficiently *in vitro* with Mg^{2+} as the divalent cation (Brown et al., 1987; Fujiwara & Mizuuchi, 1988; Ellison et al., 1990). Furthermore, the same short oligonucleotide substrate can be used as both donor and target *in vitro* with Mn^{2+} to form a gapped recombination intermediate which is the result of one integration, whereas endogenous viral DNA is not used as a target and has both ends integrated into the host genome. Accordingly, Vink et al. (1991) have stated that *in vitro* assays with short duplex DNA represent artificial systems. These discrepancies raise

† This work was supported in part by American Cancer Society Institutional Grant IRG-19.

* To whom correspondence should be addressed.

® Abstract published in *Advance ACS Abstracts,* July 1, 1995.

[1] Abbreviations: HIV-1, human immunodeficiency virus type 1; LTR, long terminal repeat; IN, integration protein (integrase); PAGE, polyacrylamide gel electrophoresis; DTT, dithiothreitol; HEPES, 4-(2-hydroxyethyl)-1-piperazineethanesulfonic acid; bp, base pair; ATP, adenosine 5′-triphosphate; MoMLV, Moloney murine leukemia virus.

0006-2960/95/0434-10205$09.00/0

concerns as to the validity of these assay systems in representing the function of IN *in vivo*.

This report describes the characterizations of endonucleolytic activity as a function of increasing DNA substrate length and DNA structural alterations. The specificity of the divalent cation requirements for both the 3′-processing and disintegration reactions are investigated. We found that increases in the length of the substrates result in a switch from Mn^{2+} to Mg^{2+} as the preferred metal cofactor for endonucleolytic activity of HIV-1 integrase. This alteration makes the reaction conditions consistent with the *in vitro* studies with endogenous viral DNA and infected cell extracts. Furthermore, we report evidence for an additional mechanism which cleaves the Y-oligomer substrate to generate the precursor form of viral DNA without regenerating target DNA.

MATERIALS AND METHODS

Protein Purification. Wild-type HIV-1 IN protein was obtained from Dr. R. Craigie. The protein was expressed in *Escherichia coli* and purified according to the procedure previously described (Sherman & Fyfe, 1990).

Oligonucleotide Substrates. Oligonucleotides containing the terminal sequence of HIV-1 DNA were synthesized and annealed to form the substrates used in this study (Chart 1). Bold letters indicate the sequences of the U5 end of the HIV-1 DNA. Oligonucleotides were purified by ethanol precipitation and electrophoresis through 20% polyacrylamide (29:1 acrylamide:bisacrylamide) denaturing gels (7 M urea). The oligonucleotide samples were electroeluted from the sliced gels using the S&S Elutrap electroseparation system from Schleicher & Schuell.

Fluorescent Labeled Substrate. 5-Amino-(12)-2′-deoxyuridine (β-cyanoethyl)phosphoramidite is a commercially available modified base that is directly introduced into oligonucleotides with a DNA synthesizer. This reagent introduces an aliphatic primary amine at the specified positions in the oligonucleotides (Lee et al., 1995). ***U*** depicts

F-D1′/T1′: 5′-TGAGTACCCGTGTGGAAAATCTCTAGCAGGGUCTATGGCGTCCCCTCTG
E-D2′: 3′-ACTCATGGGCACACCTTTTAGAGATCGTCAU

the position of the nucleotide analog. The D1′/T1′ and D2′ oligonucleotides containing this nucleotide analog were derivatized with FITC and EITC (Molecular Probes), respectively, in 100 mM $NaHCO_3/Na_2CO_3$ buffer, pH 9.0. Excess dye was removed by filtration of the reaction mixture through a Sephadex G-25 column (DNA grade). The resulting samples were then electrophoresed on denaturing (7 M urea) 20% polyacrylamide gels to further purify the oligonucleotides and to remove any residual free dyes. The appropriate oligonucleotide bands were sliced from the gels and electroeluted using the S&S Elutrap electroseparation system from Schleicher & Schuell. The fluorescent oligonucleotides were further purified by an HPLC Zorbak bio series oligo column (Du Pont).

Assays for IN Activities. One microgram of the appropriate oligonucleotide was ^{32}P-labeled at the 5′ termini by use of T4 polynucleotide kinase (New England Biolabs) and 25 μCi of adenosine[γ-^{32}P]-5′-triphosphate (3000 Ci/mmol, ICN). The labeled oligonucleotides were separated from unincorporated [γ-^{32}P]ATP using a Sephadex G-25 Quick Spin column (Boehringer Mannheim) and annealed with a 3-fold

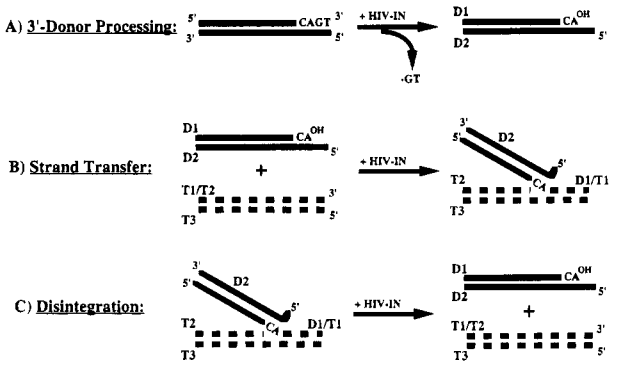

FIGURE 1: Schematic diagram of the reactions catalyzed by HIV-IN *in vitro*. (A) 3′-Donor processing. Two nucleotides are removed from the 3′-ends of the viral DNA. (B) Strand transfer. The recessed CA_{OH}-3′ end is then joined to the 5′ end of the chromosomal target DNA, producing a Y-shaped gapped recombination intermediate. (C) Disintegration. Both the precursor viral DNA and the target strand can be regenerated by a cutting−joining reaction of the Y-shaped gapped recombination intermediate. Solid lines indicate the viral donor strands (D), and dashed lines indicate the target strands (T).

molar excess of an unlabeled complementary strand in 10 mM Tris-HCl, pH 7.5, 1 mM EDTA, and 0.1 M NaCl. All the reaction mixtures for the IN protein-mediated cleavage reactions contained 25 mM HEPES, pH 7.5, 2.5 mM DTT, 50 mM NaCl, 5% glycerol (v/v), 7.5 mM Mg^{2+} or Mn^{2+}, ^{32}P-labeled substrates, and HIV-1 IN in a total volume of 20 μL. The reactions were initiated by the addition of IN and the reaction mixtures were incubated for 60 min at 37 °C. The reactions were stopped by the addition of an equal volume of stop solution (95% formamide, 30 mM EDTA, 0.1% xylene cyanol, and 0.1% bromophenol blue) to each reaction and the reactions were boiled for 5 min. A 10-μL aliquot of each reaction mixture was electrophoresed on a 7 M urea denaturing 15% (or 20%) polyacrylamide sequencing gel and the reaction products were analyzed by autoradiography. Quantitation of 3′-processing and strand transfer reaction products was performed with a Pdi densitometer Model DNA 35 using a Kodak photographic step tablet for the calibration curve.

Spectroscopic Measurements. Absorbance and absorption spectra were measured with a Hewlett-Packard 8450A diode array spectrophotometer. Steady-state fluorescence spectra and intensity were recorded with a SLM 8000 spectrophotofluorometer with 10-mm Glan-Thompson polarizers. Fluorescence emission measurements were performed under "magic angle" emission conditions (Spencer & Weber, 1970). A cuvette with a 3-mm excitation path length was used for all experiments. The absorbance of all fluorescence samples was less than 0.1 at the wavelength of excitation (460 nm) to avoid inner filter effects (Lee et al., 1995). The temperatures of the samples were regulated with a Neslab Instruments, Inc., T.E.Q. temperature controller and a PBC4 bath cooler.

The extent of cleavage was estimated by using the following equation:

$$[DNA]_c = \frac{F_t - F_0}{F_\infty - F_0} \times [DNA]_i \qquad (1)$$

where $[DNA]_c$ is the concentration of cleaved DNA, F_t is the fluorescence intensity at time t, F_∞ is the fluorescence

Chart 1

Substrate 1: 5'-CCCGTGTGGAAAATCTCTAGCAGT
3'-GGGCACACCTTTTAGAGATCGTCA

Substrate 2: 5'-TGAGTACCCGTGTGGAAAATCTCTAGCAGTGTC
3'-ACTCATGGGCACACCTTTTAGAGATCGTCA

Substrate 3: 5'-GTGTGGAAAATCTCTAGCAGGGTCTATGGCGTCC
3'-CACACCTTTTAGAGATCGT

Substrate 4: 5'-TGAGTACCCGTGTGGAAAATCTCTAGCAGGGTCTATGGCGTCCCCTCTG
3'-ACTCATGGGCACACCTTTTAGAGATCGTCA

Substrate 5: 5'-TTTAGTCAGTGTGGAAAATCTCTAGCAGGGTCTATGGCGTCCCTCTG
3'-AAATCAGTCACACCTTTTAGAGATCGTCA

Y-oligomer "A":

D1/T1 : 5'-GTGTGGAAAATCTCTAGCAGGGGCTATGGCGTCC

D2 : 5'-ACTGCTAGAGATTTTCCACAC

T2 : 5'-GAAAGCGACCGCGCC

T3 : 5'-GGACGCCATAGCCCCGGCGCGGTCGCTTTC

Y-oligomer "B":

D1'/T1' : 5'-TGAGTACCCGTGTGGAAAATCTCTAGCAGGGTCTATGGCGTCCCCTCTG

D2' : 5'-ACTGCTAGAGATTTTCCACACGGGTACTCA

T2' : 5'-GCAGGGCGAAAGCGACCGCGCC

T3' : 5'-CAGAGGGGACGCCATAGGCCCGGCGCGGTCGCTTTCGCCCTGC

Substrate C: 5'-TTTAGTCAGTGTGGAAAATCTCTAGCAGT
3'-AAATCAGTCACACCTTTTAGAGATCGTCA

Substrate D: 5'-GACCCTTTTAGTCAGTGTGGAAAATCTCTAGCAGT
3'-CTGGGAAAATCAGTCACACCTTTTAGAGATCGTCA

intensity obtained in the presence of DNase I, F_0 is the initial fluorescence intensity, and $[DNA]_i$ is the initial concentration of DNA (Lee et al., 1995). Kinetic data were analyzed using a nonlinear regression data analysis program, ENZFITTER (Elsevier-BIOSOFT).

RESULTS

There are several discrepancies between the retroviral *in vitro* and *in vivo* strand transfer reactions. The *in vitro* reaction is less efficient than the *in vivo* reaction and uses the same oligonucleotide substrate as both donor and target. Furthermore, integration products are seen predominantly *in vitro* with Mn^{2+} as the divalent cation, whereas Mg^{2+} is utilized in *in vitro* studies with endogenous viral DNA and infected cell extracts. The low efficiency of integration *in vitro* has been suggested to be due in part to the reverse of the strand transfer reaction that has been termed disintegration (Chow et al., 1992; Vincent et al., 1993). In this reaction, the unjoined 3′ end of the target strand attacks the junction between the hybrid donor and target strand and joins to the 5′ end of the cleaved target strand. This results in the precise regeneration of the 3′-end-processed donor strand and the original target strand (Figure 1). The current work focuses on determining the factors affecting donor processing activity of HIV-IN and on further examining the disintegration reaction.

It has been previously shown that substrates which contain additional base pairs (up to 4 bp) at the 3′ end of the HIV-1 U5 sequence decrease both specific cleavage and integration reactions of HIV-IN *in vitro*. However, substrates with additional nucleotides only on the processed strand next to the conserved CA-3′ (resulting in a 3′ overhang) were cleaved more efficiently than their blunt-ended counterparts (Vink et al., 1991; Mazumder et al., 1994). We hypothesized that this observed endonucleolytic activity with the 3′ overhang could have an important role in the previously reported disintegration activity of HIV-IN. The 3′ overhang may affect the donor processing activity of HIV-1 IN by the increased length of the substrate or by altering the substrate's structure.

Extensions on the 3′ End of the Processed Strand Result in Alterations of Endonucleolytic Activity. Initially, the effects of increasing the length of the processed strand on the donor processing activity were characterized. Specifically, we examined how longer 3′ overhangs, such as that which makes up the Y-intermediate, alter the 3′ donor processing activity. In each reaction, the substrates were labeled with ^{32}P at the 5′ end of the cleavable strand and incubated with purified IN in the presence of Mg^{2+} or Mn^{2+}. All of the substrates were cleaved at the phosphodiester bond after the conserved CA-3′ dinucleotide. As shown in Figure 2A, the 24-mer *substrate 1*, which mimics the U5 end of the viral DNA, was cleaved more efficiently in the presence of Mn^{2+} than Mg^{2+}. The cleavage efficiency displayed by Mn^{2+} was 41%, compared to 13% by Mg^{2+}, as determined by densitometry. This result is consistent with those that had been previously reported. The addition of 5 nucleotides 3′ to the processed strand resulted in a significant reduction in cleaved products for both divalent cations (substrate 2, Figure 2B). The cleavage efficiency with Mn^{2+} was 11% as compared to 1.4% for the Mg^{2+}-activated cleavage products, indicating that Mn^{2+} was still the preferred cation for this substrate. However, when the number of nucleotide additions was increased to 14 (substrate 3), a dramatic change in the efficiency of endonucleolytic cleavage was observed (Figure 2C). The Mn^{2+}-mediated cleavage was increased to 45% while the same substrate produced 20% cleavage with Mg^{2+}. Although Mn^{2+} was still the more efficient cofactor, the formation of cleavage products was considerably increased for both cations. This suggested that the 3′ overhang did in fact impart an effect on the activity of IN.

We further examined the endonucleolytic activity by extending both the double-stranded donor sequence at the 5′ end and the target sequence at the 3′ end (substrate 4). The length of the donor strand (D1′/T1′) was extended to a 28-mer by the addition of 9-nt random sequences at the 5′

Substrate 1: *5'-CCCGTGTGGAAAATCTCTAGCAGT
(Lane A) 3'-GGGCACACCTTTTAGAGATCGTCA
Substrate 2: *5'-TGAGTACCCGTGTGGAAAATCTCTAGCAGTGTC
(Lane B) 3'-ACTCATGGGCACACCTTTTAGAGATCGTCA
Substrate 3: *5'-GTGTGGAAAATCTCTAGCAGGGTCTATGGCGT
(Lane C) 3'-CACACCTTTTAGAGATCGTCCCAGATACCGCAGG
Substrate 4: *5'-TGAGTACCCGTGTGGAAAATCTCTAGCAGGGTCTATGGCGTCCCCTCTG
(Lane D) 3'-ACTCATGGGCACACCTTTTAGAGATCGTCA

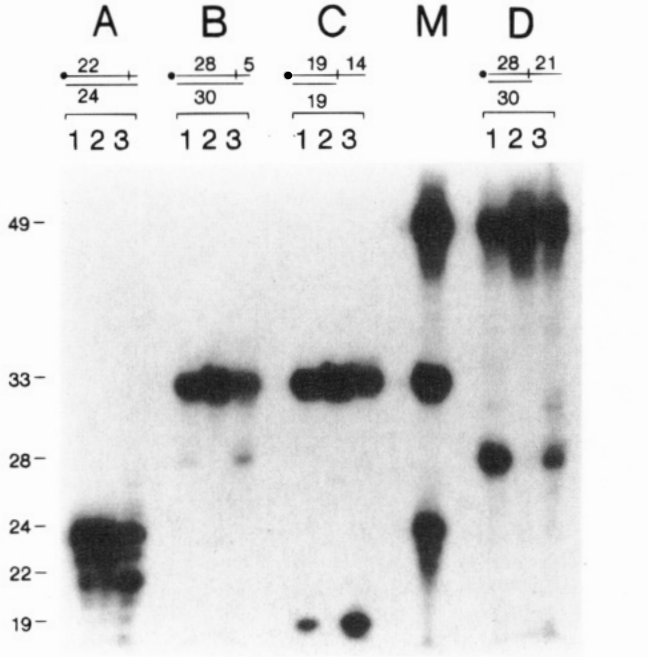

FIGURE 2: Effects of additional nucleotides to the conserved CA-3′ on HIV-1 integrase cleavage reactions. The cleavage reactions were separated by a 7 M urea denaturing 15% polyacrylamide gel and analyzed by autoradiography. The filled circle denotes the ^{32}P-labeled 5′ ends. The cleavage site and the length of each strand are indicated. (A) Substrate 1 (double-stranded 24-*mer*) corresponding to the U5 end of the HIV-1 DNA. (B) Substrate (33-mer) which contain 5 additional nucleotides next to the conserved CA-3′. (C) D1/T1 strand (33-mer) annealed to the D2 donor strand. (D) D1′/T1′ strand (49-mer) annealed to the complementary donor strand, D2′. (M) DNA size markers indicated in nucleotides on left. In panels A−D, lanes 1 and 3 represent complete reactions containing the respective substrates and integrase with 7.5 mM $MgCl_2$ and 7.5 mM $MnCl_2$, respectively. Integrase was omitted in lanes 2.

end to aid in annealing, and the target strand was increased to a 21-mer (Figure 2D). The efficiency of cleavage was 44% and 27% with Mg^{2+} and Mn^{2+}, respectively. Hence, this substrate is cleaved more efficiently with Mg^{2+} than with Mn^{2+} and shows a distinct alteration in the divalent cation preferred for the cleavage reaction. Earlier observations suggested that the 9-nt random sequences at the 5′ end should not affect the donor processing and integration activity. Vink et al. (1991) demonstrated that when all of the nucleotides at positions 14−26 were changed from T to G and A to C in the U5 end of the HIV-1 viral DNA, no effects on cleavage and integration were detected. It has been, therefore, suggested that the terminal 15 bp of the HIV-1 viral DNA are sufficient for recognition by IN (Vink et al., 1991). However, the results shown in Figure 2 suggest that changes in the length of the substrate alter both the efficiency and the preferred metal cofactor of the cleavage reaction. These results suggest that the endonucleolytic activity of HIV-1 IN is in fact substrate-length-dependent and that the extended target sequence has a role in the activity of HIV-1 IN.

Substrate 4: 5'-TGAGTACCCGTGTGGAAAATCTCTAGCAGGGTCTATGGCGTCCCCTCTG
(Lanes A) 3'-ACTCATGGGCACACCTTTTAGAGATCGTCA
Substrate 5: 5'-TTTAGTCAGTGTGGAAAATCTCTAGCAGGGTCTATGGCGTCCCTCTG
(Lanes B) 3'-AAATCAGTCACACCTTTTAGAGATCGTCA

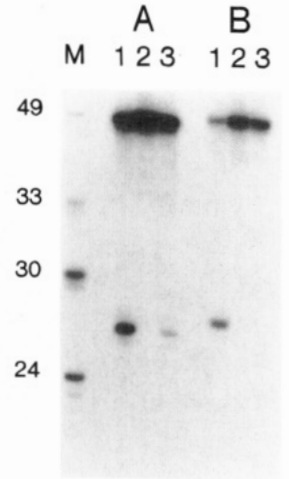

FIGURE 3: Comparison of the effects of the 9-nt random donor sequences versus the endogenous viral DNA. (A) Substrate 4 labeled on the D1′/T1′ strand. (B) Substrate 5 labeled on the 49-mer strand. The cleavage reactions were separated on a 15% denaturing polyacrylamide gel and analyzed by autoradiography. In each reaction, lanes 1 and 3 represent a complete reaction with 7.5 mM $MgCl_2$ and 7.5 mM $MnCl_2$, respectively. Lane 2 represents a reaction with no integrase.

To ensure that the observed differential activity is not an artifact of the 9 random nucleotides present at the 5′ end of the D1′/T1′ strand, the 9 nucleotides were replaced with 8 endogenous base pairs (substrate 5). This substrate displayed a similar cleavage pattern at the junction between CA and GG of the hybrid strand, regenerating the recessed donor strands (D1′/D2′) from the hybrid strands (Figure 3). The efficiencies of cleavage reactions remained better with Mg^{2+} than Mn^{2+} and were consistent with the data presented in Figure 2. Therefore, we concluded that increases in the length of both donor and target sequences in the hybrid strand result in the enhancement of activation by Mg^{2+} over Mn^{2+}.

Donor Strands Can Be Regenerated from the Intermediate Product of the in Vitro Strand Transfer Reaction by More Than One Mechanism. To determine if this differential activity was significant for the aforementioned disintegration reaction, two Y-oligomers and their related substrates were examined. Y-oligomer A consists of a 33-mer D1/T1 hybrid strand (Figure 2C), and Y-oligomer B consists of the 49-mer D1′/T1′ hybrid strand (Figure 2D). The respective Y-oligomers and their related substrates were prepared by annealing the hybrid strands to the appropriate strands.

According to the disintegration reaction (Figure 1), the ratio of the T1/T2 strand to the D1 strand should be 1:1 because production of D1 is dependent upon the formation of the T1/T2 strand. Therefore, if the Y-oligomers are labeled only on the T1/T2 strand versus only the D1 strand, the ratio of product formation should be equal. When Y-oligomer A was labeled with ^{32}P at the 5′-end of T2 (15-mer), joining of T1 (14-mer) to T2 was observed (Figure 4B). This confirms the previous disintegration data (Chow et al., 1992). This disintegration reaction is preferentially promoted by Mn^{2+}: the formation of T1/T2 product was 18 times higher with Mn^{2+} than Mg^{2+}. Similar results have been previously reported (Fesen et al., 1994). When the

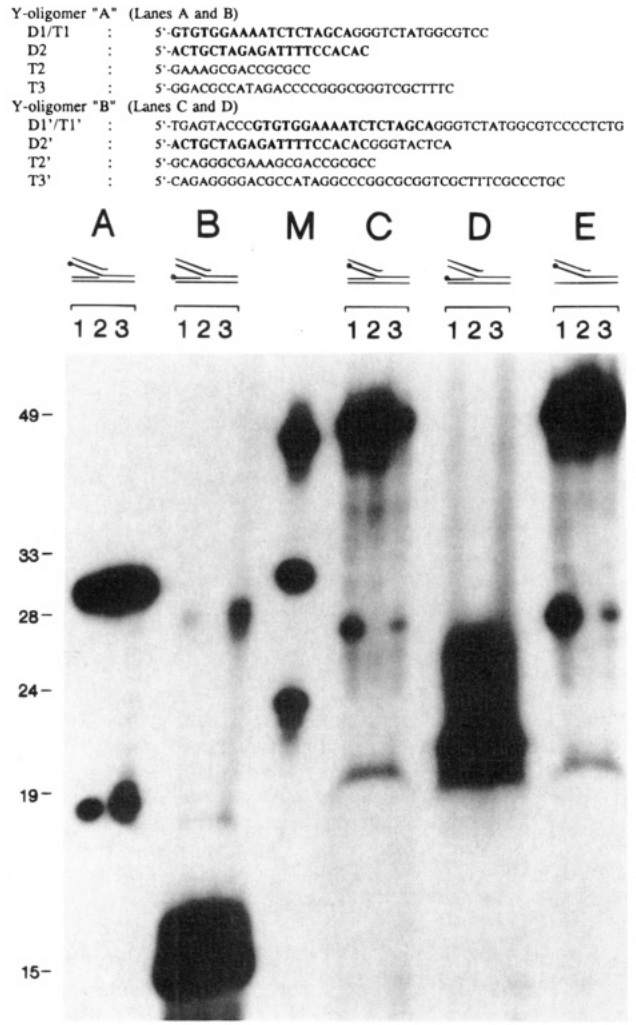

FIGURE 4: Strand cutting and joining reactions mediated by HIV-IN with various substrates. (A) Y-oligomer A radiolabeled at the 5′ end of D1/T1. (B) Y-oligomer A labeled at the 5′ end of T2. (C) Y-oligomer B labeled at the 5′ end of D1′/T1′. (D) Y-oligomer B labeled at the 5′ end of T2′. (E) Y-oligomer B minus the T2′ strand labeled at the 5′ end of D1′/T1′. (M) Molecular size markers. The cleavage reactions were separated by a denaturing 15% polyacrylamide gel and analyzed by autoradiography. In panels A−E, lanes 1 and 3 represent a complete reaction containing each substrate and integrase with 7.5 mM $MgCl_2$ and 7.5 mM $MnCl_2$, respectively. In lanes 2, integrase was omitted.

same Y-oligomer was labeled with ^{32}P at the 5′ end of the 33-mer D1/T1 (Figure 4A), similar results to the data shown in Figure 2C were observed: Mn^{2+} produced 45% cleavage product while Mg^{2+} promoted 28% cleavage. Contrary to what would be expected from the mechanism of the disintegration assay, however, these results show that the production of D1 (19-mer) is much more efficient than the regeneration of the T1/T2 strand.

Drastically different results were obtained when these experiments were repeated with Y-oligomer B as the substrate. When Y-oligomer B was labeled with ^{32}P at the 5′-end of the D1′/T1′, the results were consistent with the data observed in Figure 2D, which favored Mg^{2+} over Mn^{2+} (Figure 4C). The extent of the cleavage products was 12% with Mg^{2+} and 5% with Mn^{2+}. These results were confirmed in nondenaturing polyacrylamide gels (data not shown). Furthermore, when this Y-oligomer was labeled at the 5′ end of T2′ (22-mer), T1′/T2′ products were not observed in the presence of either Mn^{2+} or Mg^{2+} (Figure 4D).

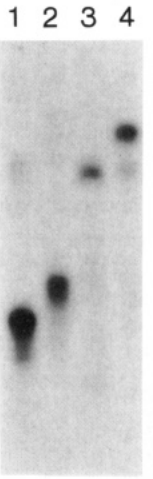

FIGURE 5: Analysis of annealed substrates. Substrates were annealed as previously described (see Materials and Methods). All substrates were annealed with ^{32}P-labeled D1′/T1′. Upon annealing, each substrate was analyzed on a TBE 10% polyacrylamide gel. Lane 1 contains D1′/T1′. Lane 2 contains D1′/T1′ annealed to D2′. Lane 3 contains the three-stranded substrate of D1′/T1′, T3′, and D2′. Lane 4 is the complete Y-oligomer B substrate, the strand transfer intermediate.

Since the disintegration reaction requires T2′ (or T2), the product strand D1′ should not be produced from a three-stranded substrate which lacks the T2′ strand. Cleavage reactions with Y-oligomer B minus the T2′ strand (Figure 4E) showed that the quantity of cleaved product of D1′ was 27% with Mg^{2+} and 7% with Mn^{2+}. Hence, D1′ was produced more efficiently than with the original Y-oligomer (Figure 4C), as if a different activity was cleaving the hybrid strand.

To ensure that the observed cleavage product (D1 strand) from three- and four-stranded substrates was not from the two-stranded substrate due to incomplete annealing, the integrity of each of the substrates was tested by native polyacrylamide gel electrophoresis. Autoradiography data after electrophoretic separation ensured the absence of unannealed strands as shown in Figure 5. All of the substrates were completely or nearly completely annealed. Therefore, the results shown in Figure 4 cannot be accounted for by the presence of incompletely annealed substrates. These results with both Y-oligomers are not accounted for by the previously described disintegration reaction and suggest that the integrase protein differentially recognizes DNA substrates depending on their structures and that this recognition is further differentiated by the different divalent cations. We concluded that a distinctively different disintegration mechanism must exist which cleaves the Y-oligomer into the original donor strand without producing the original form of the target strand.

Accordingly, we hypothesized that the D1 and D1′ strands were being predominantly produced from the Y-oligomers by a different mechanism which results in cleavage of the hybrid strands. The 3′ donor processing reaction precisely cleaves between the CA and GT at both ends of the HIV-1 linear DNA, whereas the disintegration reaction takes place precisely in between the CA and GG in the Y-oligomer substrate. A slight difference in the terminal 3′ nucleotide in these sequences does not seem to be significant for these reactions since it has been shown that HIV-1 integrase can catalyze the donor processing of both the HIV-1 (CAGT)

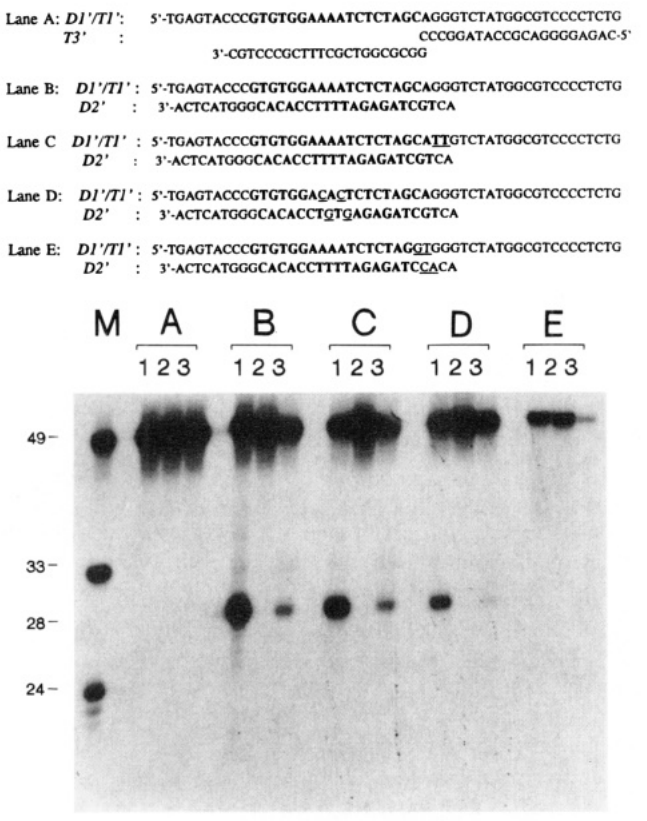

FIGURE 6: Effects of alterations in the nucleotide sequence on the cleavage reaction mediated by HIV-IN. (A) D1′/T1′ strand (49-mer) annealed to T3′. (B) D1′/T1′ substrate (49-mer). (C) CAGG in the D1′/T1′ strand replaced by CATT. (D) AAAA sequence in the D1′/T1′ strand altered to ACAC. (E) CAGG in the D1′/T1′ strand changed to GTGG. Substrates in panels B−E were annealed to their appropriate complementary strands. (M) Molecular size markers. The cleavage reactions were separated by a denaturing 15% polyacrylamide gel and analyzed by autoradiography. In panels A−E, lanes 1 and 3 represent a complete reaction containing each substrate and integrase with 7.5 mM $MgCl_2$ and 7.5 mM $MnCl_2$, respectively. In lanes 2, integrase was omitted.

and HIV-2 (CAGG) substrates with equal efficiency (van Gent, 1991). It could therefore be envisioned that endonucleolytic cleavage by the IN protein at the CA site (Figure 2) regenerates the D1′/D2′ and D1/D2 substrates without producing the T1′/T2′ and T1/T2 strands. This alternative mechanism, shown in Figure 11, would explain why the T1′/T2′ strand was not produced when the D1′ strand was regenerated from the Y-oligomer.

Endonuclease Properties of HIV-1 Integrase. To confirm the authenticity of the Mg^{2+}-dependent endonucleolytic activity of HIV-IN, various substrates were analyzed for their cleavage efficiency. If radiolabeled D1′/T1′ is annealed to the T3′ strand without the D2′ and T2′ strands, cleavage products should not be detected since there is no recognition site for HIV-IN. Figure 6A shows that products are not formed in the presence of either cation. Cleavage products were also not observed with either metal when the T3′ strand was radiolabeled at the 5′ end and annealed to the D1′/T1′ strand (data not shown). Differences in the cleavage pattern were not observed when the sequence CAGG within the D1′/T1′ strand was replaced by the sequence CATT found at both ends of the MoMLV DNA (Figure 6C). Both substratesshowed identical 39% cleavage with Mg^{2+} and 14% cleavage with Mn^{2+}, in good agreement with previous fluorescence data (Lee et al., 1995). However, when the

Substrate C: 5′-TTTAGTCAGTGTGGAAAATCTCTAGCAGT
(Lanes A) 3′-AAATCAGTCACACCTTTTAGAGATCGTCA
Substrate D: 5′-GACCCTTTTAGTCAGTGTGGAAAATCTCTAGCAGT
(Lanes B) 3′-CTGGGAAAATCAGTCACACCTTTTAGAGATCGTCA

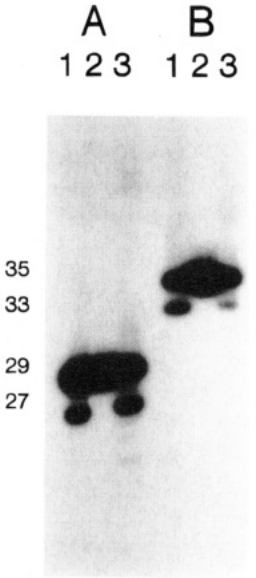

FIGURE 7: Analysis of substrate length dependence on donor processing activity. (A) Substrate C (29-mer) labeled on the processing strand. (B) Substrate D (35-mer) labeled on the processing strand. All cleavage reactions were separated by a denaturing 15% polyacrylamide gel and analyzed by autoradiography. In both panels, lanes 1 and 3 represent complete reactions with 7.5 mM $MgCl_2$ and 7.5 mM $MnCl_2$, respectively. Lanes 2 represent a reaction with no integrase.

AAAA tract within the D1′/T1′ strand was replaced by the sequence ACAC, 17% and 7% cleavage efficiencies with Mg^{2+} and Mn^{2+} were observed, respectively (Figure 6D), as compared to those shown in Figure 6B. As expected, no cleavage products were detected when the sequence CAGG present in the D1′/T1′ strand was substituted with GTGG (Figure 6E). These results confirm that both donor strands containing specific sequences necessary for donor processing by HIV-1 integrase are required for the observed cleavage activity. These endonuclease activities are analogous to those that would be associated with the 3′ donor processing activity. Therefore, it is highly conceivable that the 3′ donor processing activity of HIV-IN is also substrate-length-dependent. We hypothesized that the observed endonuclease activity of HIV-1 integrase is directly related to the sequence-specific 3′ end cleavage activities and that HIV-1 IN would display similar substrate-length-dependent donor processing activities.

Substrate-Length-Dependent Donor Processing Activity of HIV-1 Integrase. To further test whether Mg^{2+}-dependent endonuclease activity is accounted for by the donor processing activity, substrates C and D were prepared. These substrates contain 29 and 35-mer donor strands, respectively, which correspond to the U5 end of HIV-1 DNA. The target sequences were omitted. The cleavage reactions of substrate C (Figure 7A) showed both Mg^{2+} and Mn^{2+}-dependent cleavage patterns with approximately equal efficiency: 28% cleavage with Mg^{2+} and 30% cleavage with Mn^{2+}. This result supports the data shown in Figure 2 and 4, although there is a slight difference in the extent of cleavage. These results also suggest that there is a further role for the extended target sequence in the activity of HIV-IN and that there is a

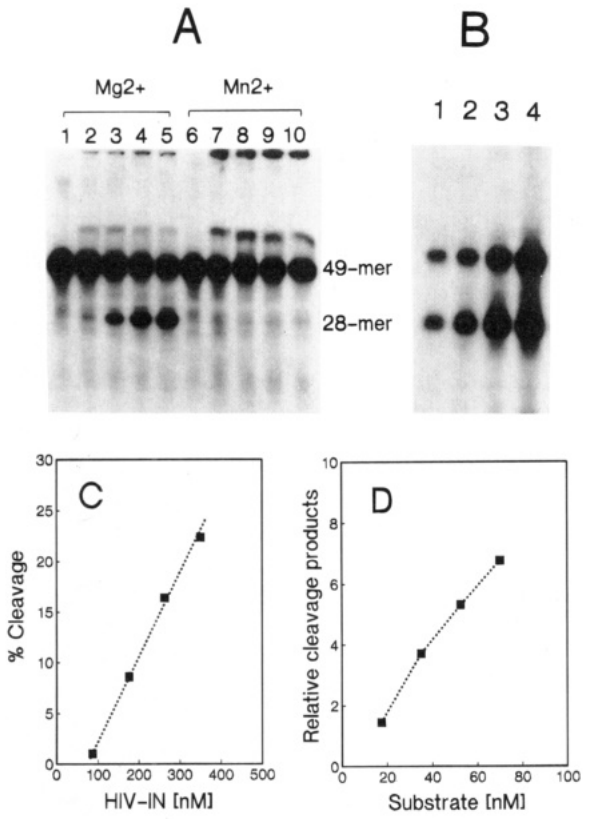

FIGURE 8: Analysis of enzyme and substrate concentration-dependent cleavage reaction performed with ^{32}P-labeled D1′/T1′ annealed to D2′. (A) Lanes 1−5 and 6−10 represent reactions performed with 1 pmol of substrate in the presence of 7.5 mM $MgCl_2$ and 7.5 mM $MnCl_2$, respectively. In lanes 1 and 6, integrase was omitted. The concentrations of IN used in lanes 2−5 and 7−10 were 88, 175, 263, and 350 nM, respectively. (B) The concentrations of substrates used were 17.5, 35, 53, and 70 nM, respectively, with 225 nM enzyme. The entire reaction mixtures were electrophoresed on a 7 M urea denaturing 20% polyacrylamide gel (16-cm × 14-cm plates) and analyzed by autoradiography. (C, D) Gel data were scanned by using a densitometer and the quantitated data were plotted and represent the results shown in panels A and B, respectively.

substrate-length-dependent donor processing activity. This was further supported from the cleavage reaction with 35-mer substrate D (Figure 7B). The degree of cleavage was higher in the presence of Mg^{2+} than Mn^{2+}: 33% with Mg^{2+} and 16% with Mn^{2+}. It should be emphasized that the predominant Mg^{2+}-dependent donor processing activity was not observed from shorter oligonucleotide substrates as shown in Figure 2A. Therefore, we conclude that Mg^{2+}-dependent activity is enhanced with increasing substrate length, whereas the Mn^{2+}-dependent activity shows an opposite effect. The substrate-dependent differential donor processing activity seems responsible for the alterations in the cleavage activity observed in Figure 2.

Fluorescence Kinetic Studies of the Mg^{2+}-Dependent 3′-Processing Activity of HIV-IN. The Mg^{2+}-dependent cleavage reaction *in vitro* with substrate 4 was further characterized as a function of both substrate and enzyme concentration. As shown in Figure 8A, increasing amounts of product formation were observed with increasing concentrations of the enzyme in the presence of Mg^{2+}. Substrate concentrationdependence was also observed with Mg^{2+} as the catalytic cofactor (Figure 8B). The gel data shown in Figure 8 (panels A and B) were scanned using a densitometer and the resulting data were plotted as shown in Figure 8 (panels C and D). These results indicate that the cleavage reaction of substrate 4 shows a linear response to the enzyme concentration. Moreover, increasing substrate concentrations yield increasing amounts of cleavage products, suggesting that this substrate is a good candidate for *in vitro* kinetic studies.

This led us to prepare a fluorogenic substrate which contains a fluorescence donor and acceptor as shown in Chart 2. Both FITC and EITC were covalently labeled to the primary amine group of the nucleotide analog U, 5-amino-(12)-2′-deoxyuridine (β-cyanoethyl)phosphoramidite. Significant resonance energy transfer from fluorescein to eosin (calculated Förster distance is 54 Å; Carraway et al., 1989) is expected from this fluorogenic substrate due to the strong spectral overlap between the emission spectrum of fluorescein (λ_{MAX} = 520 nm) and the absorption spectrum of eosin (λ_{MAX} = 525 nm). Utilizing this substrate, we have previously characterized the endonucleolytic activity of HIV-IN using fluorescence resonance energy transfer (FRET; Lee et al., 1995). The fluorescence assay was confirmed by direct comparison of fluorescence data to those obtained by autoradiography analysis of the cleavage reaction with radiolabeled fluorogenic substrate. Our results indicate that the intensity ratio of the donor fluorescence in the the absence of its energy acceptor to that in its presence is approximately 8:1. Since HIV-1 IN usually displays a low cleavage efficiency, one advantage of utilizing FRET is that it enhances the detection of substrate cleavage. For example, 10% cleavage of the substrate would result in approximately a 2-fold increase in the fluorescence intensity.

The kinetics of the DNA cleavage reactions were monitored with excitation and emission wavelengths of 460 and 510 nm, respectively. These wavelengths were chosen to avoid the contribution from the eosin (acceptor) fluorescence. Time-dependent cleavage reactions were monitored by the enhancement of the donor fluorescence at 510 nm and the initial velocities were determined from the linear portion of these curves. The extent of IN-mediated DNA cleavage was determined from the recovery of the donor fluorescence as compared to DNase I digestion of the same concentration of substrate. Since DNase I results in the complete digestion of the fluorogenic substrate, the resultant donor fluorescence from DNase I digestion can be used as the reference for the total recovered donor fluorescence. Alternatively, the fluorescence intensity of the donor labeled single-stranded DNA can be used as the control. We chose to use digestion by DNase I as the control in order to rule out any intensity variation due to incomplete annealing of the substrate.

To test whether HIV-IN exhibits concentration-dependent differential activation of Mg^{2+}-catalyzed 3′-processing activity, fluorescence kinetic studies were performed as a function of HIV-IN concentration with a fixed concentration of the fluorogenic substrate (40 nM) in this current study. Figure 9 shows the plot of the initial velocity vs enzyme concentration (from 45 to 540 nM). This resulted in a linear plot, suggesting that the rate of cleavage was first-order with respect to the HIV-IN concentration. However, no activity was detected at concentrations lower than 45 nM HIV-IN, indicating that subunit interactions may be required for activity (Jones et al., 1992). The same results were also obtained from the Mg^{2+}-dependent activity with 25 nM radiolabeled substrate (Figure 8, panels A and C). The characteristics of the first-order kinetics suggest that the

Chart 2

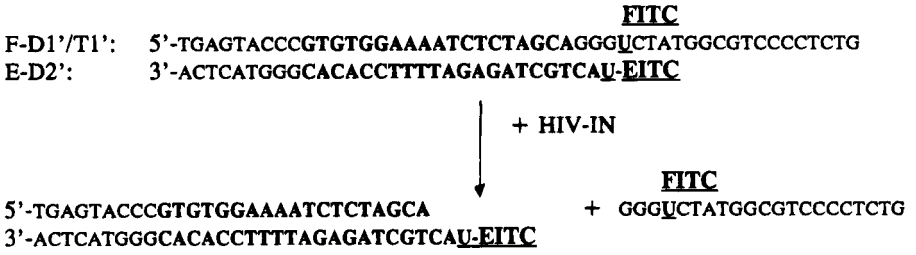

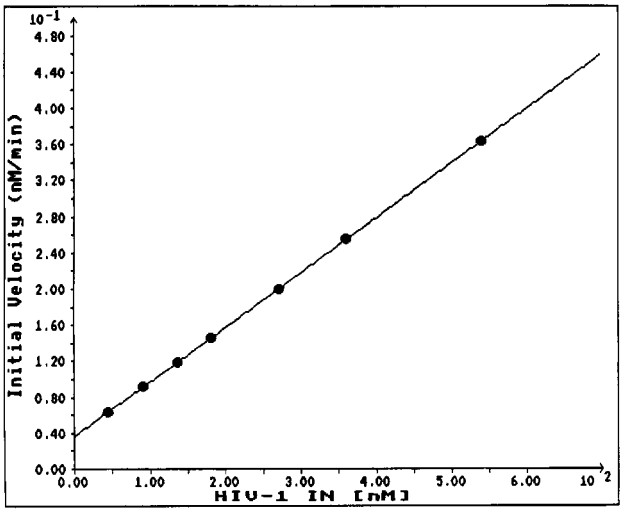

FIGURE 9: A plot of initial velocity vs HIV-IN concentration. The kinetic experiments were performed with a fixed concentration of fluorogenic substrate, 40 nM. The HIV-IN concentrations were varied from 45 to 540 nM. Fluorescence intensity was monitored with excitation and emission wavelengths of 460 and 510 nm, respectively. The initial velocities of cleavage reactions were determined from the linear portions of the kinetic data.

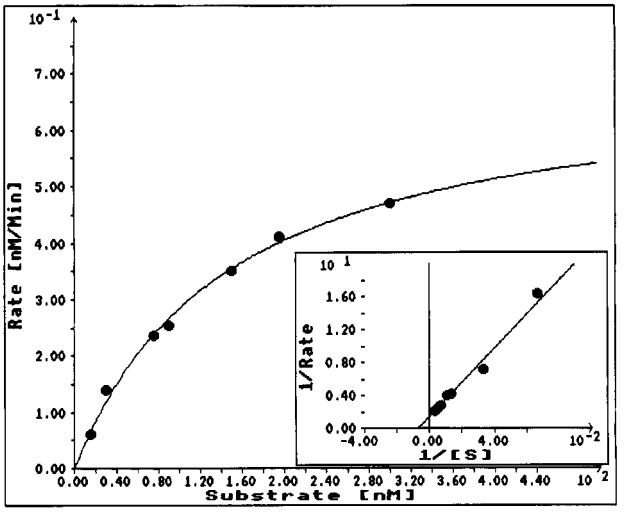

FIGURE 10: A plot of initial velocity vs [S] and a Lineweaver–Burk plot (inset). The kinetic experiments were performed with a fixed concentration of HIV-IN, 174 nM. The substrate concentration was varied from 15 to 300 nM. Fluorescence intensity was monitored with excitation and emission wavelengths of 460 and 510 nm, respectively. The initial velocities were determined from the linear portions of the cleavage reactions. Inset: A Lineweaver–Burk plot of the same data.

enzyme activity is not dependent on the protein concentration in this range but that the actual active enzyme concentration is much lower than the enzyme added to the reaction mixture. It is conceivable that the low enzyme activity is due to the low solubility of HIV-1 IN in the reaction mixture containing 50 mM NaCl.

To obtain kinetic parameters, assays were performed in which the substrate concentration (from 15 to 300 nM) was varied with a fixed concentration of HIV-1 IN (174 nM). Figure 10 shows a plot of initial velocity vs [S] and a Lineweaver–Burk plot (inset). The apparent V_{max} under these reaction conditions is 0.7 ± 0.04 nM/min, which gives a turnover number (k_{cat}) for the cleavage reaction of 0.004/min for an IN monomer. The apparent K_m is 145 ± 17 nM, which yields $k_{cat}/K_m = 2.3 \times 10^5$ M^{-1} min^{-1} for an IN monomer. The k_{cat} estimated in this study indicates that HIV-1 IN turns over 0.24 times for a 60-min reaction time. One interpretation of this low k_{cat} is that the protein does not turn over during the 3′-processing reaction. In fact, a typical reaction shows that 5 pmol of the enzyme cleaves 10–30%of a 0.5-pmol DNA sample in 60 min. There is no experimental data showing complete cleavage of substrate in any conditions. Hence, this incomplete and low enzyme activity of HIV-1 IN may be due to the very low catalytic turnover.

DISCUSSION

Substrate Structure and Length Dependence on Endonucleolytic Activity. 3′ Donor processing characterized with a short oligonucleotide substrate shows that HIV-1 IN catalyzes the reaction with a preference for Mn^{2+} over Mg^{2+} (Vincent et al., 1993). This characteristic has been observed with other retroviral IN proteins. MoMLV and avian IN proteins are much more efficient in cleaving the viral DNA with Mn^{2+}, although the avian IN protein maintains greater selectivity in the presence of Mg^{2+}. This implied that Mg^{2+} is required for optimal specificity even though the activity is reduced (Katzman et al., 1989; Vink et al., 1991). A similarity between the MoMLV, avian, and HIV-1 integrases is that two nucleotides are precisely removed from the 3′ ends of the viral DNA (Grandgenett & Mumm, 1990). Cleavage occurs next to the conserved terminal CA-3′ and subsequently exposes the CA_{OH}-3′. A minimal length of 15 base pairs from the termini of duplex DNA, which contains the corresponding sequence of the viral DNA ends, is also required for specific cleavage (Katzman et al., 1989). Single base substitutions of the terminal GT-3′ to GG or TT do not significantly alter the efficiency of cleavage (van Gent et al., 1991), but single base substitutions of the conserved CA sequence to TA resulted in the total inhibition of cleavage activity (Bushman & Craigie, 1991). Thus, retroviral integrases exhibit similar substrate specificity and require Mn^{2+} as the preferred metal cofactor when short oligonucleotide substrates are utilized for their *in vitro* reactions. However, as demonstrated in the current study, the endonucleolytic activity is altered to a Mg^{2+}-dependent activity with longer substrates.

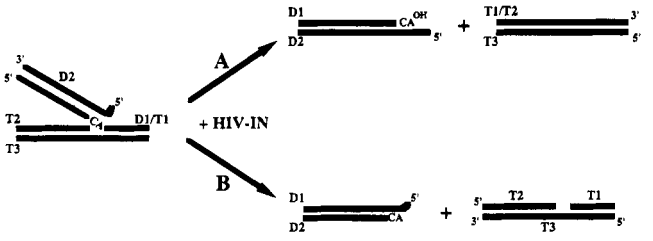

FIGURE 11: Schematic diagram of two different mechanisms of disintegration. (A) Disintegration. The OH-3′ of the cleaved target DNA attacks the junction between the donor/target hybrid strand of the Y-shaped substrate to regenerate the donor and rejoin the target strands. (B) Alternative disintegration. The presence of the proximal target DNA as the source of the nucleophile is not required. Presumably, water or glycerol is used as a nucleophile to cleave the hybrid strand. Therefore, this mechanism is catalyzed by the sequence-specific 3′-processing activity and not accompanied by a cutting−joining reaction of the target strands.

The endonuclease activity responsible for regenerating the donor strands from the Y-oligomer substrate correlates directly with the donor processing activity of HIV-1 IN. This conclusion was drawn from the following observations: the endonuclease activity is metal-dependent and cleaves between CA and GG. When the sequence CAGG is changed to CATT, the same precise cut is observed immediately following the conserved CA-3′. No cleavage is observed from the single-stranded substrate or from the Y-oligomer in the absence of the D2 strand. When the conserved CA sequence is replaced by GT, the cleavage activity is completely abolished. Therefore, these properties of endonuclease activity are identical to those of the donor processing activity: as the length of the donor sequences was increased, the endonuclease activity that cleaves specifically between the donor and target sequence of the hybrid strands and 3′ donor processing displayed Mg^{2+}-dependent activity.

Significance of Alternative Disintegration. The Mg^{2+}-dependent activity of HIV-IN also plays a significant role in distinguishing the two different mechanisms that can regenerate the donor strands from Y-substrates (Figure 11). According to previous mechanistic studies (Engelman et al., 1991), the strand transfer reaction requires HIV-1 IN to arrange the CA_{OH}-3′ of the cleaved viral donor DNA to the target DNA in such a way that the resulting CA_{OH}-3′ attacks the target DNA to produce a Y-shaped intermediate. In the disintegration reaction, the OH-3′ of the cleaved target DNA attacks the junction between the donor/target hybrid strand of the Y-shaped substrate to regenerate the donor and rejoin the target strands. Thus, the disintegration reaction has been suggested as the reverse reaction of strand transfer. Both strand transfer and disintegration reactions are activated by Mn^{2+} but not by Mg^{2+}, indicating that both activities are correlated. Chow et al. (1992) further suggested that the inefficient integration reaction observed *in vitro* can be accounted for in part by the counteracting effect of the disintegration. However, these two reactions do not always show a direct correlation. Mutant integrase proteins lacking both the 3′-processing and strand transfer activities have been shown to catalyze the disintegration activity (Engelman & Craigie, 1992; Vincent et al., 1993; Engelman et al., 1993; Leavitt et al., 1993).

As demonstrated in this study, the ratio of the regenerated donor (D1 or D1′) and target (T1/T2 or T1′/T2′) strands from the Y-shaped substrates are not the same, indicating that the D1 and D1′ strands were not regenerated exclusively by the disintegration reaction. We propose that an alternative mechanism, herein referred to as alternative disintegration, cleaves the junction between the viral and target DNA sequences. This mechanism differs from the previously described disintegration in its deficiency of a concerted cutting−joining reaction. In contrast to disintegration, alternative disintegration is catalyzed by the sequence-specific 3′-processing activity. Thus, this mechanism does not require the presence of the proximal target DNA as the source of the nucleophile but presumably uses water or glycerol as a nucleophile to cleave the hybrid strand in accordance with previous chemical characterizations (Engelman et al., 1991). Depending on the length of the substrates, this reaction can be activated by either divalent cation, Mg^{2+} or Mn^{2+}. The 3′-processing activity responsible for the regeneration of D1′ donor strand from Y-oligomer B (longer substrate) was preferentially activated by Mg^{2+}, whereas the shorter Y-oligomer "A" substrate was more efficiently cleaved by Mn^{2+}. It is apparent that the efficiency of the Mg^{2+}-dependent 3′-processing activity increases as the length of substrate increases and decreases as the DNA substrates are altered from the two-stranded DNA to the four-stranded Y-oligomer substrate, an indication that HIV-IN differentially recognizes DNA substrates depending on their length and structure. Interestingly, both Y-oligomers (A and B) and related substrates did not produce the strand transfer products. This suggests that the strand transfer products may be cleaved by the 3′-processing activity of HIV-IN, thereby reducing the efficiency of strand transfer reaction. Although it is presently unknown whether alternative disintegration reactions occur *in vivo*, its possibility makes it important to obtain a better understanding of this reaction in order to elucidate the mechanism of the overall integration process. Further characterization is necessary since the Mg^{2+}-dependent reaction not only catalyzes the alternative disintegration of the Y-oligomer substrates but also may be biologically relevant with respect to the cleavage and integration of viral DNA *in vivo*. Moreover, the absence of alternative disintegration would indicate that a mechanism exists *in vivo* which prevents this process to achieve the efficient integration.

An important factor determining the overall integration reaction could be the structural requirements of the DNA substrates. Local and global changes in DNA structures often alter binding affinity of the proteins. It is also conceivable that the protein may undergo conformational changes due to binding to the different structures of the DNA substrates, resulting in significant alterations in the functional properties of the protein. HIV-IN will most likely face significant changes in DNA structure during the entire process of retroviral integration. For a better understanding of the substrate-dependent differential activation of HIV-IN, DNA binding affinities associated with different lengths of DNA substrates must be examined along with the differential effects of the two divalent cations, Mg^{2+} and Mn^{2+}. Therefore, characterization of the effects of structural changes of DNA substrates on functional properties of HIV-IN is the topic of future investigation.

Kinetic Studies of the Mg^{2+}-Dependent 3′-Processing Activity of HIV-IN. Designing a fluorogenic substrate made it possible to characterize the cleavage kinetics by fluorescence resonance energy transfer. This led us to develop an

in vitro fluorescence assay which is rapid, simple, continuous, and nonradioactive (Lee et al., 1995). This fluorescence assay made it easier for kinetic studies of the 3′-processing activity of HIV-IN. The results from the fluorescence studies (Figures 9 and 10) correlated well with those obtained from gel electrophoresis analyses (Figure 8) validating the use of the fluorescence assay towards kinetic studies.

This kinetic study provided an interesting catalytic turnover number. The V_{max} (0.7 nM/min) and the total enzyme concentration (174 nM) gave a k_{cat} of 0.004/min or 0.24/h. This result suggests that HIV-IN requires 4 h to turn over. This apparent low turnover implies that HIV-IN may remain bound to DNA following the removal of the two nucleotides from the viral DNA. Consequently, HIV-IN may direct the exposed CA_{OH}-3′ into the proper orientation and proximity to the target DNA to promote the concerted phosphoryl transfer. This mechanistic model is consistent with the results of previous mechanistic studies (Engelman et al., 1991). Thus, integrase would only be dissociated from the DNA following the strand transfer reaction and thereby turn over. The kinetic data obtained from this study, however, differ from those of RSV-IN. Previous kinetic studies indicate that RSV-IN efficiently turns over (0.52/min for an IN dimer) (Jones et al., 1992). It is possible that HIV-IN used in this study does not have a high specific activity due to the low concentration of the protein which may not efficiently form a functional dimeric enzyme. This can be attributed to the lower solubility of HIV-IN at low salt conditions. HIV-IN exhibits a limited solubility even at 1 M NaCl (<0.5 mg/mL). Since not all of the integrase added to the reaction mixture is expected to be soluble, it is possible that only a small fraction of the total integrase protein is active, which would reduce the activity of the enzyme and result in a lower catalytic turnover. Although this possibility cannot be ruled out, the lower turnover indicates that the majority of HIV-IN remains as a complex. The observation that preintegration complexes of HIV-IN/DNA can exist stably for prolonged periods of time support this assertion (Ellison & Brown, 1994). Nevertheless, further kinetic studies are crucial in determining and verifying the mechanism of the overall viral integration process.

Conclusion. The completion of retroviral integration may not be accomplished by retroviral IN alone. It is probable that the host DNA repair system plays an important role in the integration process. Further studies are needed to determine if retroviral or cellular proteins other than IN have a direct role in this integration process. It will be a tremendous advantage to gain a complete understanding of those factors that regulate viral integration.

The Mg^{2+}-dependent *in vitro* activity of HIV-1 integrase provides a better understanding of the structural and functional properties of HIV-1 integrase. Longer substrates that correspond more to the endogenous viral DNA alter the function of HIV-1 IN to bring the *in vitro* reaction in better agreement with the *in vivo* reaction. Our results indicate that there are additional roles for the extended sequences and that these sequences are in fact important for the *in vivo* function of the enzyme. In this manner, Mg^{2+}-dependent activities may be better suited to screen for specific inhibitors of HIV-1 integrase.

ACKNOWLEDGMENT

We thank R. Craigie for his helpful comments and careful reading of the manuscript.

REFERENCES

Bowerman, B., Brown, P. O., Bishop, J. M., and Varmus, H. E. (1989) *Genes Dev. 3*, 469−478.
Brown, P. O., Bowerman, B., Varmus, H. E., and Bishop, J. M. (1987) *Cell 49*, 347−356.
Brown, P. O., Bowerman, B., Varmus, H. E., and Bishop, J. M. (1989) *Proc. Natl. Acad. Sci. U.S.A. 86*, 2525−2529.
Bushman, F. D., and Craigie, R. (1991) *Proc. Natl. Acad. Sci. U.S.A. 88*, 1339−1343.
Bushman, F. D., Fujiwara, T., and Craigie, R. (1990) *Science 249*, 1555−1558.
Carraway, K. L., III, Koland, J. G., and Cerione, R. A. (1989) *J. Biol. Chem. 264*, 8699−8707.
Chow, S. A., Vincent, K. A., Ellison, V., and Brown, P. O. (1992) *Science 255*, 723−726.
Craigie, R., Fujiwara, T., and Bushman, F. (1990) *Cell 62*, 829−837.
Ellison, V., and Brown, P. O. (1994) *Proc. Natl. Acad. Sci. U.S.A. 91*, 7316−7320.
Ellison, V., Abrams, H., Roe, T., Lifeson, J., and Brown, P. O. (1990) *J. Virol. 64*, 2711−2715.
Engelman, A., Mizuuchi, K., and Craigie, R. (1991) *Cell 67*, 1211−1221.
Farnet, C. M., and Haseltine, W. A. (1990) *Proc. Natl. Acad. Sci. U.S.A. 87*, 4164−4168.
Fesen, M. R., Pommier, Y., Leteurtre, F., Hiroguchi, S., Yung, J., and Kohn, K. W. (1994) *Biochem. Pharmacol. 48*, 595−608.
Fujiwara, T., and Mizuuchi, K. (1988) *Cell 54*, 497−504.
Fujiwara, T., and Craigie, R. (1989) *Proc. Natl. Acad. Sci. U.S.A. 86*, 3065−3069.
Grandgenett, D. P., and Mumm, S. R. (1990) *Cell 60*, 3−4.
Jones, K. S., Coleman, J., Merkel, G. W., Laue, T. M., and Skalka, A. M. (1992) *J. Biol. Chem. 267*, 16037−16040.
Katz, R. A., and M. Skalka (1994) *Annu. Rev. Biochem. 63*, 133−73.
Katz, R. A., Merkel, G., Kulkosky, J., Leis, J., and Skalka, A. M. (1990) *Cell 63*, 87−95.
Katzman, M., Katz, R. A., Skalka, A. M., and Leis, J. (1989) *J. Virol. 63*, 5319−5327.
Leavitt, A. D., Shiue, L., and Varmus, H. E. (1993) *J. Biol. Chem. 268*, 2113−2119.
Lee, S. P., Censullo, M. L., Kim, H. G., Knutson, J. R., and Han, M. K. (1995) *Anal. Biochem. 227*, 295−301.
Mazumder, A., Engelman, A., Craigie, R., Fesen, M., and Pommier, Y. (1994) *Nucleic Acids Res. 22*, 1037−1043.
Pauza, C. D. (1990) *Virology 179*, 886−889.
Sherman, P. A., and Fyfe, J. A. (1990) *Proc. Natl. Acad. Sci. U.S.A. 87*, 5119−5123.
Spencer, R. D., and Weber, G. (1970) *J. Chem. Phys. 52*, 1654−1663.
van Gent, D. C., Elgersma, Y., Bolk, M. W. J., Vink, C., and Plasterk, R. H. A. (1991) *Nucleic Acids Res. 19*, 3821−3827.
Varmus, H. E. and Brown, P. O. (1989) Retrovirus, in *Mobile DNA* (Berg, D. E., & Howe, M. M., Eds.) pp 53−108, American Society for Microbiology, Washington, DC.
Vincent, K. A., Ellison, V., Chow, S. A., and Brown, P. O. (1993) *J. Virol. 67*, 425−437.
Vink, C., van Gent, D. C., Elgersma, Y.; and Plasterk, R. H. A. (1991) *J. Virol. 65*, 4636−4644.
Vora, A. C., Fitzgerald, M. L., and Grandgenett, D. P. (1990) *J. Virol. 64*, 5656−5659.

BI950171U